# C by Michael Mehring

# Nuclear magnetic resonance in high- $T_c$ superconductors

This paper is aimed at the nonspecialist in nuclear magnetic resonance who wants to know what NMR can do to increase his understanding of high- $T_{\rm c}$  superconductors. Most NMR results are discussed in an illustrative manner to facilitate intuitive understanding. Several specific NMR experiments are presented which demonstrate the variety of this experimental technique. Special emphasis is given to the following aspects: ionic charges and quadrupole interaction, local fields and magnetic ordering, conduction electrons and Knight shifts, quasiparticle excitations, and nuclear spinlattice relaxation.

### 1. Introduction

In this paper we wish to demonstrate that nuclear magnetic resonance is one of the most important tools for the investigation of high- $T_{\rm c}$  superconductors [1]. In classical superconductors NMR has already played a decisive role [2–4]. One of the highlights was the demonstration of gap opening and quasiparticle excitation by nuclear spin-lattice relaxation in <sup>27</sup>Al [2, 3]. This was one of the strongest supports for the theory of Bardeen, Cooper, and Schrieffer (BCS). It is interesting to note that the same phenomena

<sup>©</sup>Copyright 1989 by International Business Machines Corporation. Copying in printed form for private use is permitted without payment of royalty provided that (1) each reproduction is done without alteration and (2) the *Journal* reference and IBM copyright notice are included on the first page. The title and abstract, but no other portions, of this paper may be copied or distributed royalty free without further permission by computer-based and other information-service systems. Permission to *republish* any other portion of this paper must be obtained from the Editor.

were observed by means of nuclear spin-lattice relaxation of <sup>139</sup>La in La<sub>1.8</sub>Sr<sub>0.2</sub>CuO<sub>4</sub> [5]. Besides these nuclear spin relaxation phenomena, there is a wealth of information contained in NMR experiments. A review of NMR experiments on classical superconductors given by McLaughlin [4] is highly recommended for further reading.

The following is restricted to a few specific cases in which NMR has been applied to high- $T_{\rm c}$  superconductors. Section 2 deals with structural information obtained from quadrupolar spectra. Since magnetism plays an important role, hyperfine fields and magnetic ordering are discussed in Section 3. In the normal state, high- $T_{\rm c}$  superconductors show the typical metallic effects known as Knight shifts, discussed here. However, they are strongly modified by magnetic correlations, and this is treated in Section 4. Finally, nuclear spin-lattice relaxation and its connection with BCS gap opening are discussed in Section 5.

# 2. Structural information from quadrupole spectra

The measurement of electrical field gradients ( $V_{xx}$ ,  $V_{yy}$ ,  $V_{zz}$ ) at a particular site in a crystalline solid by zero-field nuclear quadrupole resonance (NQR) and high-field NMR is well established. The only prerequisite is a nucleus with spin I > 1/2 and quadrupole moment  $Q \ne 0$ . In high- $T_c$  superconductors there are plenty of those. Among the first nuclei investigated were <sup>63</sup>Cu (I = 3/2;  $\gamma/2\pi = 11.285$  MHz/T;  $eQ = 0.211 \times 10^{-24}$  cm<sup>2</sup>), <sup>65</sup>Cu (I = 3/2;  $\gamma/2\pi = 12.040$  MHz/T;  $eQ = -0.195 \times 10^{-24}$  cm<sup>2</sup>), and <sup>189</sup>La (I = 7/2;  $\gamma/2\pi = 6.014$  MHz/T;  $eQ = 0.2 \times 10^{-24}$  cm<sup>2</sup>).

Let us begin with Cu NQR/NMR in YBa<sub>2</sub>Cu<sub>3</sub>O<sub>7</sub>. Mali et al. [6] were among the first who observed Cu NQR as well as

NMR spectra in this superconductor. Others obtained very similar results [7–11] and confirmed the initial assignment of Mali et al. concerning the two different Cu sites in  $YBa_2Cu_3O_7$ , namely Cu(1) for the CuO chains, with a quadrupole frequency  $\nu_Q$  near 22 MHz, and Cu(2) for the CuO<sub>2</sub> planes, with a quadrupole frequency near 31 MHz.

For a spin I = 3/2, it is well known that the  $\pm 1/2 \rightarrow \pm 3/2$  transitions are degenerate and result in a single NQR line [12] at

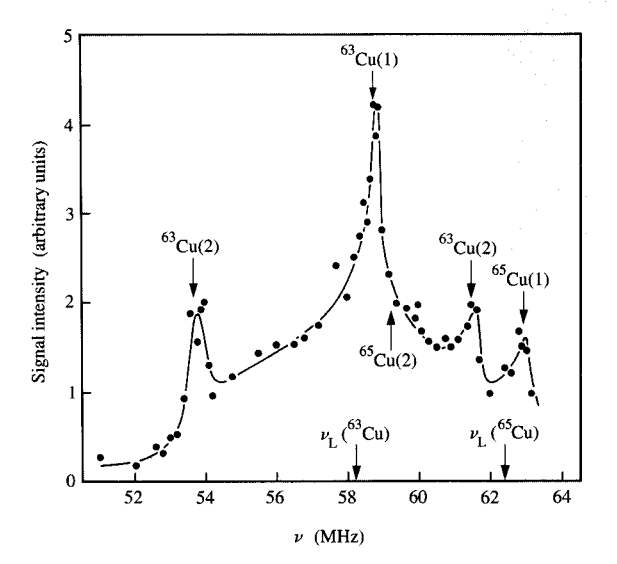
$$\nu_{Q} = \frac{eQ}{2h} V_{zz} \left( 1 + \frac{1}{3} \eta^{2} \right)^{1/2}, \tag{1}$$

where the asymmetry parameter  $\eta = (V_{xx} - V_{yy})/V_{zz}$  cannot separately be determined in zero field. It is therefore necessary to apply a high magnetic field  $B_0$ , where all four levels (I = 3/2) are split. This results in a central transition  $(-1/2 \rightarrow 1/2)$  near the Larmor frequency  $\nu_1$ , and two "satellite transitions" at  $\nu_L \pm \nu_O(\vartheta, \phi)$  which now depend strongly on the Euler angles  $(\phi, \vartheta)$  of the magnetic field with respect to the principal axis system of the field-gradient tensor [12]. As a result, the satellite transitions are broadened so much that they are unobservable in YBa<sub>2</sub>Cu<sub>3</sub>O<sub>7</sub> and only the central transition is observed. Even the central transition is drastically broadened by secondorder quadrupole interaction, as is shown in Figure 1 [6(a)]. Moreover, both isotopes <sup>63</sup>Cu and <sup>65</sup>Cu are visible in the spectrum. More recently, the spectra shown in Figure 2 have demonstrated the combination of NQR and NMR spectra in the superconducting samples of YBa<sub>2</sub>Cu<sub>3</sub>O<sub>6</sub> [11]. The information obtained from both NQR and NMR leads to the determination of  $V_{-}$  and  $\eta$ .

These values are very distinct for the two Cu sites. Whereas  $\eta \approx 0$  for the Cu(2) site, as might be expected from just considering the local symmetry of Cu(2) ( $V_{xx} = V_{yy}$  in the plane),  $\eta \approx 1$  for the Cu(1) chain site [6-11, 13]. Mali et al. [6] and, more recently, Riesenmeier et al. [14] have used a point-charge model to account for the different asymmetry parameters and the absolute value of  $V_{-}$  at Cu(1). Figure 3 gives a pictorial representation of the point charges which best fit the experimental data [6]. The following values were obtained [6]:  $\eta$  [Cu(1)] = 0.92 experimental and 0.98 calculated, whereas  $v_Q$  [Cu(1)] = 22 MHz experimental and 21.3 MHz calculated. However, the agreement between experiment and the point-charge calculation might be fortuitous, and a more elaborate quantum-mechanical calculation seems to be required. In this sense the point charges quoted might be viewed as "fictitious" charges. Nevertheless, they give important information on the different local symmetries of the Cu(1) and Cu(2) sites.

# 3. Local fields and magnetic ordering: Hyperfine broadenings and splittings

In this section we wish to demonstrate that NQR/NMR has contributed much to the understanding of magnetic ordering

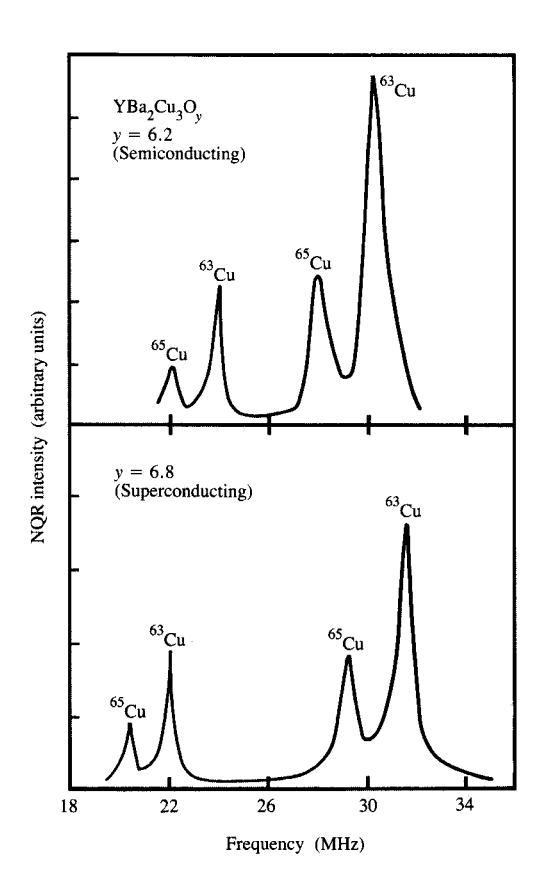


### Entities.

The Cu NMR spectrum of YBa $_2$ Cu $_3$ O $_7$  at 300 K according to Mali et al. [6(a)]. A constant external magnetic field of 5.17 T was applied.  $\nu_L$  is the Larmor frequency of the respective Cu isotope. Special spectral features have been assigned to the Cu(1) (chains) and Cu(2) (planes) sites, respectively.

and correlations in this class of materials. Figure 4 shows the NQR spectra of La<sub>2</sub>CuO<sub>4</sub> by Kitaoka et al. [15(a)]. Since Kitaoka presents their work in more detail in his paper in this issue [15(b)], we discuss it only briefly. Figure 4 demonstrates clearly that all possible NQR transitions of the  $I = 7/2^{139}$ La spin can be observed, allowing determination of the electric field gradient at the La site. Moreover, each line is split because of a local field which arises from the antiferromagnetic ordering originating at the Cu sites in La<sub>2</sub>CuO<sub>4</sub>. Such quadrupole splittings and local hyperfine fields in La<sub>2-x</sub>(Sr, Ba), CuO<sub>4</sub>-type solids have been observed by different groups [15-17]. The splitting of the lines is directly related to the antiferromagnetic order parameter. This is demonstrated in Figure 5 [17], where the linesplitting can be followed up to the Néel temperature  $T_N$  in different samples in this class of materials [15-17]. Others have observed the same effect, and a number of interesting investigations have appeared dealing with antiferromagnetic ordering in  $La_{2-x}(Sr, Ba)_x CuO_4$  [15–17].

NQR/NMR has helped considerably in establishing the phase diagram which is schematically sketched in **Figure 6**. Aharony et al. [18] discuss the physics of this phase diagram in more detail; we confine ourselves here to a specific spinlattice relaxation phenomenon which has been observed in  $\text{La}_2\text{CuO}_{4-y}$  [19, 20]. Oxygen and La defects in  $\text{La}_2\text{CuO}_4$  may



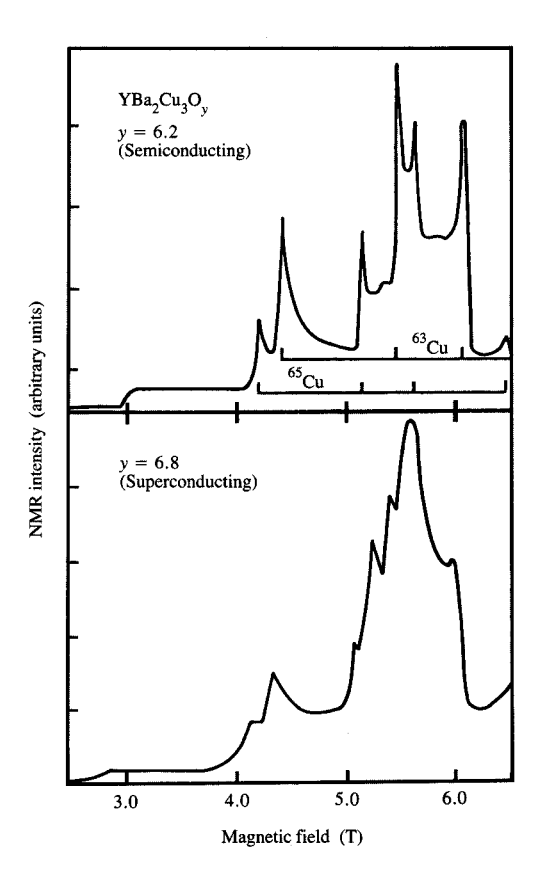


Figure 2

NQR and NMR (at 64 MHz) spectra of YBa<sub>2</sub>Cu<sub>3</sub>O<sub>y</sub>, with y = 6.2 (top) and y = 6.8 (bottom) at 4.2 K by Lütgemeier [11]. Assignments of the spectral peaks to the <sup>63,65</sup>Cu isotopes are indicated.

lead to the introduction of holes into the CuO, layers in a manner similar to Sr, Ba doping. It is therefore expected that even a nominal La<sub>2</sub>CuO<sub>4</sub> sample does not correspond to X = 0 in Figure 6, where X is taken here as the concentration of holes. When cooling such a sample, one may proceed along a path indicated by the downwardpointing arrow in Figure 6. Although the phase diagram shows basically antiferromagnetic behavior, there is a rapid increase in spin-lattice relaxation at low temperatures, as is evident from Figure 7 [20]. Two characteristic temperatures occur, namely  $T_{\rm c1} \simeq 4.8~{\rm K}$  and  $T_{\rm c2} \simeq 60~{\rm K}$ . At both temperatures there is an increase in the  $T_2$  relaxation rate, which basically samples the extremely slow motion of the antiferromagnetic order parameter. The critical increase of the relaxation rate at  $T_{c1} \simeq 4.8 \text{ K}$  is, however, seen by both  $T_1$  and  $T_2$ . Both nuclear spin-lattice relaxation times  $T_1$  and  $T_2$  are in this case very sensitive monitors of extremely slow motion (in the kHz to MHz range) of the antiferromagnetic

order parameter. They indicate that at both temperatures  $T_{c1}$ and  $T_{\rm c2}$  new magnetic states appear within the antiferromagnetic domain. These might be the "spincanting" of the copper electron spins ( $T_{c2} = 60 \text{ K}$ ) and the re-entrant spin-glass transition ( $T_{c1} \simeq 4.8 \text{ K}$ ). Details of these phenomena will be published elsewhere [20(b)]. It is interesting to note, also, that the class of materials such as YBa<sub>2</sub>Cu<sub>3</sub>O<sub>3</sub> exhibits a phase diagram very similar to the one presented in Figure 6. Especially for y = 6 (O<sub>6</sub>), the material is antiferromagnetic. This has been nicely demonstrated by Yasuoka et al. [21], whose results are shown in Figure 8. A strong hyperfine field of about 7 T corresponding to 90 MHz for the Zeeman splitting resides on the Cu(2) sites, whereas it is absent at the Cu(1) sites. The Cu(1) sites just show the typical NQR spectrum of  $^{65}$ Cu ( $\nu_{\rm O} = 28$  MHz) and  $^{63}$ Cu  $(\nu_{\rm O} = 30 \text{ MHz})$ , which is drastically shifted from where it was for y = 7 (O<sub>2</sub>), namely around 22 MHz. This indicates that the oxygen defects occur predominantly in the Cu(1) chains.

At intermediate y the situation is slightly different and can be followed quite nicely by NMR [22]. More detailed information has come from NMR than from neutron-scattering experiments in these materials [22].

# 4. Conduction electron spins: Knight shifts and Korringa relation

The shift of an NMR line with respect to the bare nuclear Larmor frequency  $\nu_1$  can be expressed [12] as

$$\nu = \nu_1 (1 + \delta), \tag{2}$$

where the total shift  $\delta$  comprises basically two different contributions in metals:

$$\delta = K_{\rm spin} + K_{\rm orb} + \sigma. \tag{3}$$

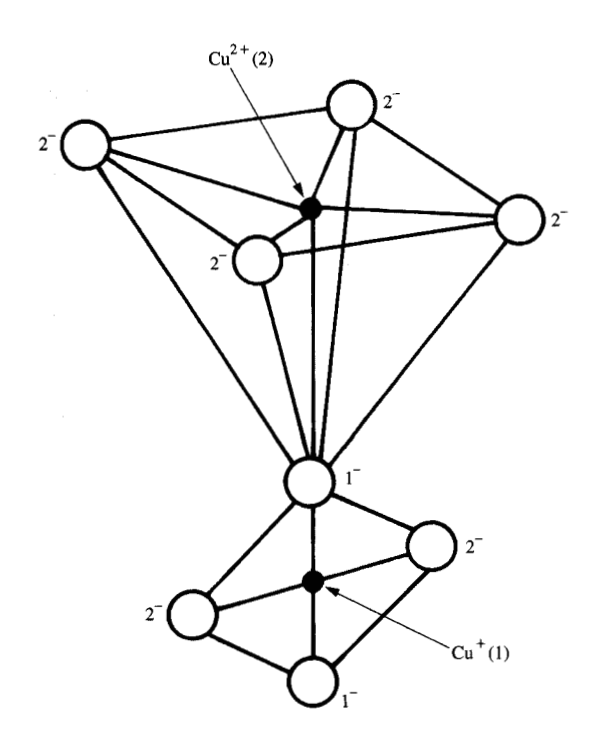
Here the Knight shifts  $K_{\rm spin}$  and  $K_{\rm orb}$  are due to the conduction electrons, whereas the chemical shift  $\sigma$  is caused by the residual orbitals not contributing directly to the conduction band. In metals the Knight shifts are usually the dominant contribution to the total shift, and the chemical shift can be subtracted by choosing a suitable nonmetallic reference compound. We restrict ourselves in the following to the Knight shifts, which may be expressed as

$$K_{zz} = \frac{A_{zz}^{(\text{spin})}}{\hbar \gamma_{e} \gamma_{n}} \chi_{\text{spin}}(T) + \frac{A_{zz}^{(\text{orb})}}{\hbar \gamma_{e} \gamma_{n}} \chi_{\text{orb}}, \tag{4}$$

where  $A_{zz}$  is the hyperfine component parallel to the external magnetic field  $(B_0 \parallel z)$ ,  $\chi$  is the susceptibility per electron, and  $\gamma_e$ ,  $\gamma_n$  are the gyromagnetic ratios of electrons and nuclei, respectively. The orientational dependence of  $K_{zz}$  follows that of  $A_{zz}$  and is well known for second-rank tensors

$$K_{zz} = K_{11} \sin^2 \beta \cos^2 \alpha$$
  
  $+ K_{22} \sin^2 \beta \sin^2 \alpha + K_{33} \cos^2 \beta,$  (5)

where  $(K_{11}, K_{22}, K_{33})$  are the principal elements of the Knight-shift tensor, and the Euler angles  $(\alpha, \beta)$  denote the orientation of the magnetic field with respect to the principal axis system. In contrast to ordinary cubic metals, a strong Knight-shift anisotropy is expected in high- $T_c$ superconductors. To cite the "Knight shift" alone is thus not sufficient. In fact, Knight shifts have been observed in YBa<sub>2</sub>Cu<sub>2</sub>O<sub>7</sub> [6-11, 13]. Whereas Mali et al. [6] in their original paper quote the Knight shifts Cu(1),  $K \simeq 10^{-2}$ , and Cu(2),  $K \approx 0.66 \times 10^{-2}$ , single-crystal studies have more recently become available [13] with the result for  $B_0 \parallel c$ : Cu(1),  $K \simeq 0.6 \times 10^{-2}$  and Cu(2),  $K \simeq 1.25 \times 10^{-6}$ . The apparent disagreement between these data is nicely resolved in a very recent investigation by the Los Alamos group [23], who used a magnetically oriented powder to study the orientation and temperature dependence of the Knight shift in YBa<sub>2</sub>Cu<sub>3</sub>O<sub>2</sub>. Figure 9 presents their data for the Knightshift anisotropy. From these studies [23] one obtains the



### Maria Prince A

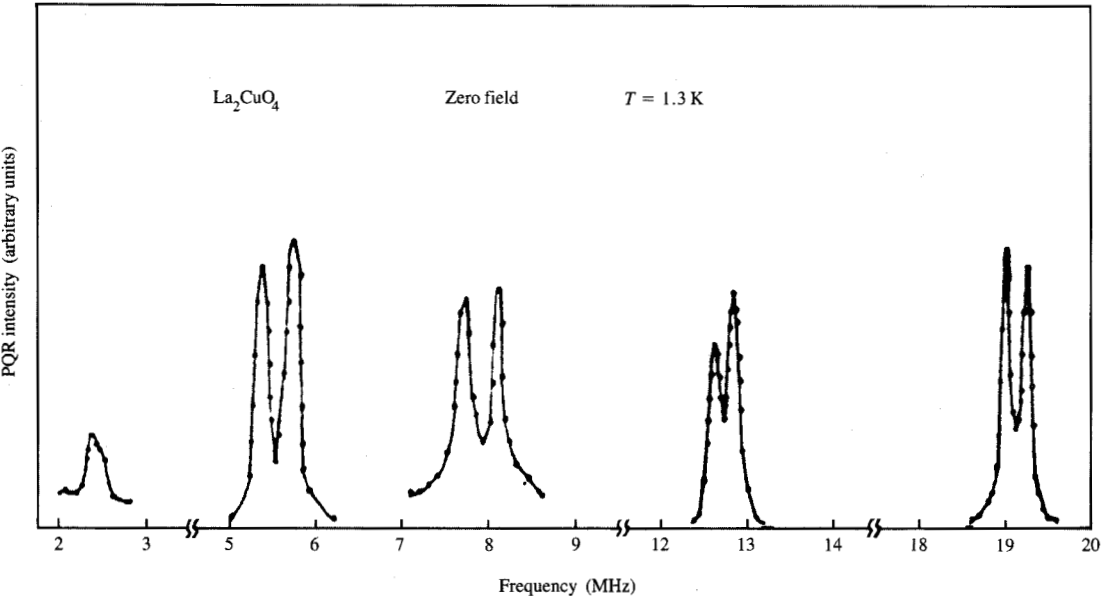
Pictorial representation of the copper-oxygen skeleton in the YBa<sub>2</sub>Cu<sub>3</sub>O<sub>7</sub> unit cell. Chain Cu(1) and plane Cu(2) sites are labeled correspondingly. The charges indicated follow the point-charge model according to [6], as discussed in the text.

Knight-shift tensors  $(K_a, K_b, K_c) = (0.6, 1.35, 0.6) \times 10^{-2}$  for Cu(1) and  $(0.6, 0.6, 1.25) \times 10^{-2}$  for Cu(2) with basically the same isotropic part  $K_{iso} = (K_a + K_b + K_c)/3 \approx 0.8 \times 10^{-2}$ .

Both Knight-shift tensors are essentially identical except for different orientations of the principal axis, which is parallel to the b-axis for Cu(1) and parallel to the c-axis for Cu(2). It is interesting to note that a similar relation holds for the electric field gradient (see Section 2). However, the essential facts about the Knight shift are that first of all the Cu Knight shift in YBa<sub>2</sub>Cu<sub>3</sub>O<sub>7</sub> is 6–7 times larger than in metallic copper, although the conductivity in the superconductor above  $T_c$  is much smaller than for metallic copper and also is practically the same for the Cu(1) and Cu(2) sites. However, this does not prove that the conduction mechanisms are identical for Cu(1) and Cu(2).

Before discussing this further, let us briefly take a look at the copper spin-lattice relaxation. A number of reports on nuclear spin-lattice relaxation  $(T_1)$  of the two copper sites [Cu(1) and Cu(2)] showing essentially the same behavior have appeared in the literature recently [6-10, 24]. The





Zero-field (NQR) spectrum of  $^{139}$ La in La<sub>2</sub>CuO<sub>4</sub> at 1.3 K according to Kitaoka et al. [15]. All possible allowed nuclear spin (I=7/2) transitions are observed. The line splittings result from the hyperfine field caused by the antiferromagnetic ordering.

relaxation rate in the metallic regime  $(T > T_c)$  is much stronger than in metallic copper and behaves differently for Cu(1) and Cu(2). Both again do not follow the typical Korringa relation [12]

$$K^2T_1T = \text{const.} ag{6}$$

In fact, a more general form of the Korringa relation can be derived [25] as

$$K^2 T_1 T \times C_0 S_K = 1, \tag{7}$$

$$C_0 = \frac{4\pi k_{\rm B}}{\hbar} \left(\frac{\gamma_{\rm n}}{\gamma_{\rm s}}\right)^2,\tag{8}$$

with  $S_{\kappa} = 1$  for the 3D free-electron gas. When the dimensionality of the electron dynamics becomes less than 3D,  $S_{\kappa} > 1$  is expected. In highly one-dimensional solids  $S_{\rm K}$  can reach values of the order of 80 [25]. Moreover,  $S_{\rm K}$ can become temperature-dependent due to a change in the temperature-dependent spectral density in highly correlated systems. It should be noted that the observation of a Knight shift and a Korringa-like relation is not a unique signature of a metal. On the contrary, the same relations hold as well for an insulator, provided it is magnetic and has rapidly

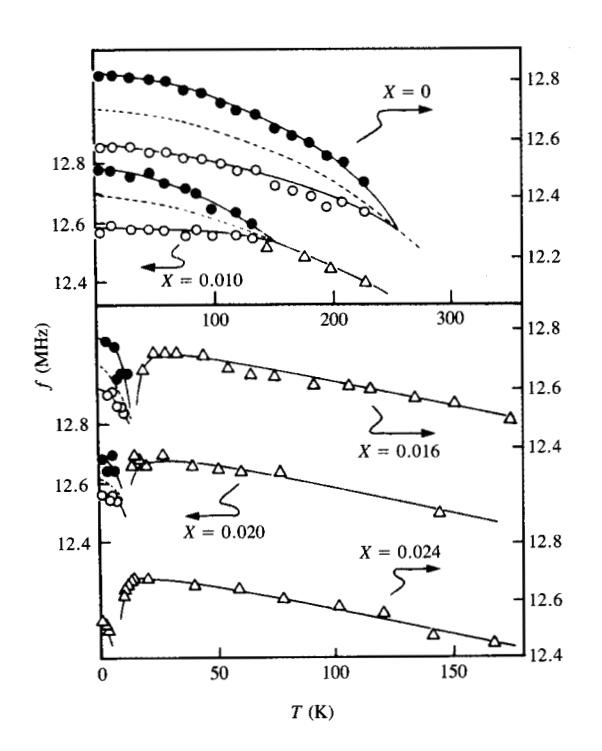
exchanging spins governed by a large exchange-coupling constant J. For both cases the Korringa relation can be derived from the more general expression [26]

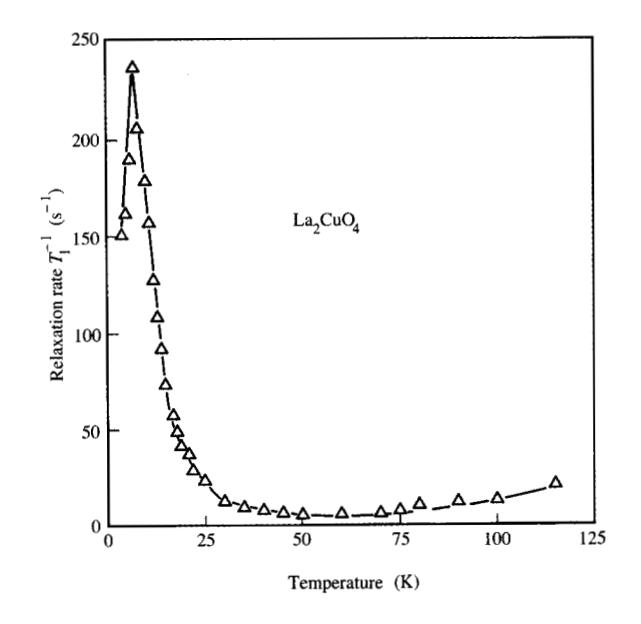
(6) 
$$\frac{1}{T_{1}} = \frac{2k_{\rm B}T}{\hbar^{2}} \sum_{q} A_{q} A_{-q} \frac{\chi^{\perp}(q, \omega_{\rm n})}{\omega_{\rm n}},$$
 (9)

where  $A_a$  is the spatial Fourier transform of the electronnuclear interaction and  $\chi^{\perp}(q, \omega)$  is the imaginary part of the transverse dynamic susceptibility. It is therefore quite reasonable that the large Knight shift and the strong spinlattice relaxation of Cu in YBa<sub>2</sub>Cu<sub>3</sub>O<sub>7</sub> are caused not by the holes on the oxygen sites, which are responsible for the conduction, but rather by the electron spins residing on Cu<sup>2+</sup>(2). The strong antiferromagnetic fluctuations on the Cu(2) sites, due to the exchange-coupling constant J, "modulate" the hyperfine interaction A with the nuclear spins. According to the Anderson exchange model [27], a "back-of-the-envelope" calculation yields for the nuclear spin relaxation rate [28]

$$\frac{1}{T_{1,2}} = 0.64 \, \frac{\Delta \omega^2}{J} \,, \tag{10}$$

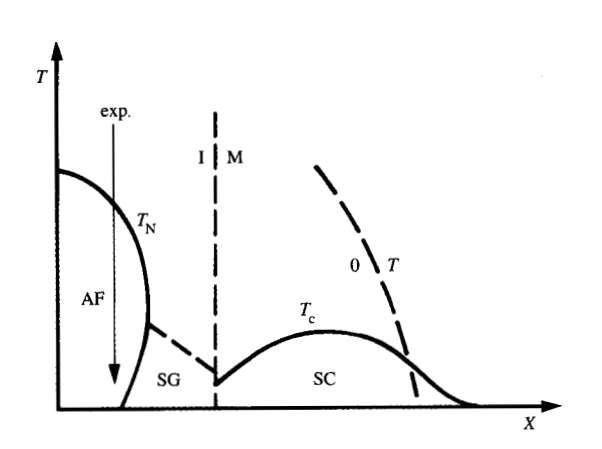
where  $\Delta \omega = A/2$ . A reasonable estimate of A leads to  $\Delta \omega = 2\pi \times 1.25 \times 10^8 \text{ rad-s}^{-1}$ . With  $T_1 \simeq 400 \ \mu\text{s}$  (for T =

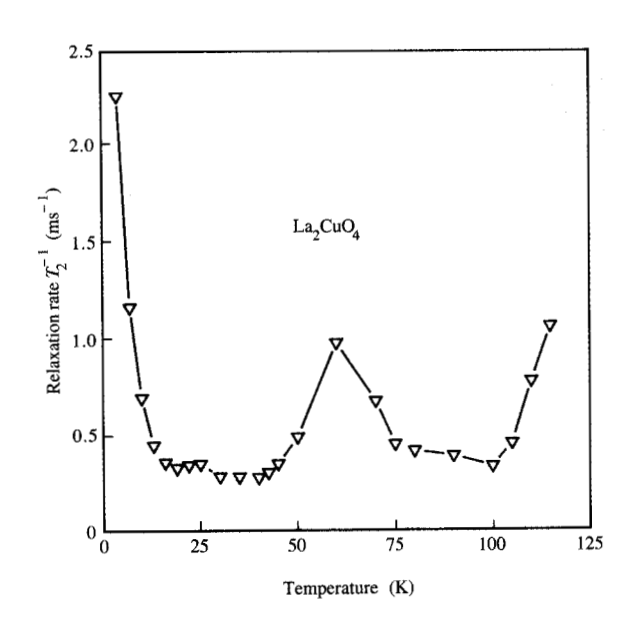




### Figure 5

Temperature variation of line splittings of the  $^{139}$ La NQR lines in  $\text{La}_{2-x}$  Ba<sub>x</sub>CuO<sub>4</sub> according to Watanabe et al. [17] for different x values. The magnetic phase diagram was determined by this technique.

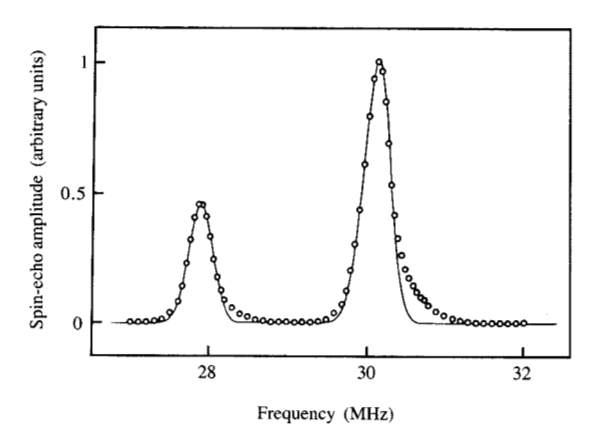


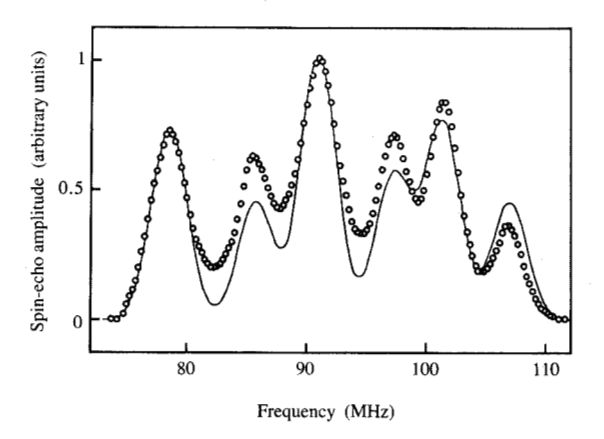


### Figure 6

Schematic phase diagram of the  $\text{La}_{2-x}(\text{Sr, Ba})_x \text{CuO}_4$  system (see Aharony et al. [29(b)]). The following symbols apply: AF, antiferromagnetic; SG, spin glass; SC, superconducting; I, insulator; M, metal. The vertical arrow indicates a path followed in an experiment shown in Figure 7.

Nuclear spin relaxation rates  $1/T_1$  (top) and  $1/T_2$  (bottom) of  $^{139}$ La in La<sub>2</sub>CuO<sub>4- $\delta$ </sub> versus temperature performed at zero field according to Hentsch et al. [20].

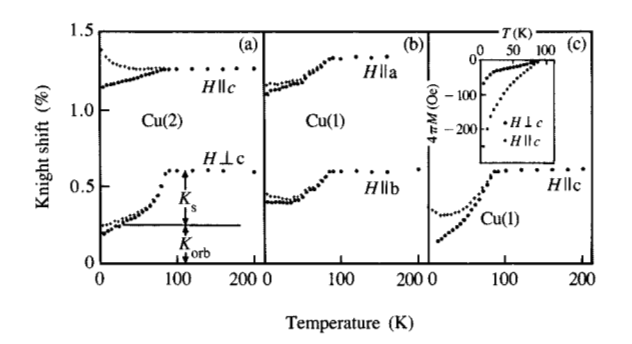




### annin:

NMR spectra of Cu nuclei in  $YBa_2Cu_3O_6$  in zero external field according to Yasuoka et al. [21]. Top: Quadrupole line of  $^{65}$ Cu (28 MHz) and  $^{63}$ Cu (30 MHz) of the Cu(1) site at 4.2 K. Bottom: Local field shifted Cu lines at Cu(2) site observed at 1.3 K.

100–120 K), one arrives at  $J \approx 100$  meV, which comes close to similar values obtained from completely independent measurements (see K. B. Lyons et al., Z. Schlesinger, and A. Aharony et al. [29]). Although a more quantitative analysis is necessary, it seems to be evident that the Cu relaxation is governed by antiferromagnetic correlations rather than conducting holes. This view is also supported by the completely different relaxation behavior observed for <sup>17</sup>O in YBa<sub>2</sub>Cu<sub>3</sub>O<sub>7</sub> [30]. In view of these results, the Cu Knight shift has to be interpreted as a "pseudo-Knight shift" in the sense that it is caused by antiferromagnetic exchange. Since hyperfine interaction may be transferred between Cu(2) and Cu(1) via the pyramidal oxygen, this could be the reason for similar Knight shifts of Cu(1) and Cu(2).



### HINTY W

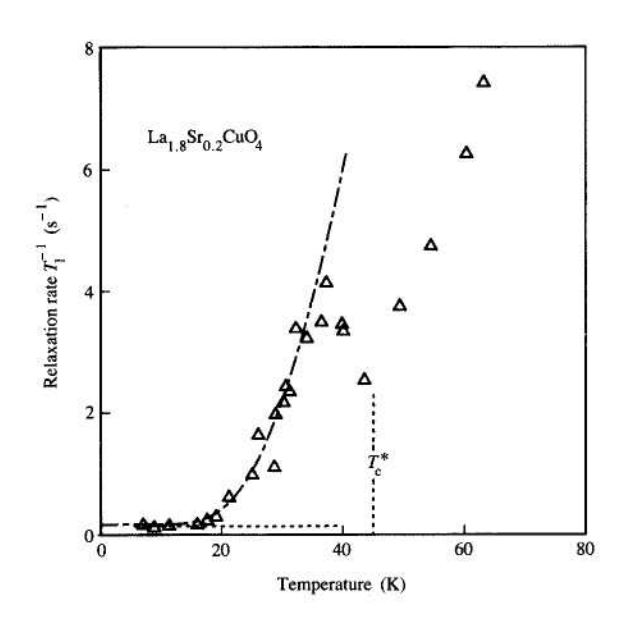
Temperature variation of the anisotropic  $^{63}$ Cu Knight shift in YBa<sub>2</sub>Cu<sub>3</sub>O<sub>7</sub> according to Takigawa et al. [23(b)]. The "raw" Knight shifts (•) were corrected for demagnetizing and shielding effects (+). The insert in (c) shows the temperature variation of the magnetization.

In the superconducting state, the Cu Knight shift decreases with decreasing temperature, as is expected for spin pairing. However, as shown in Figure 9, the Knight shift does not vanish completely, as would be expected for BSC-like superconductivity. Nevertheless, Equation (4) tells us that even if the spin susceptibility went to zero, the temperatureindependent orbital contribution could account for the residual Knight shift. It is, however, surprising that the orbital contribution should be so large. It might therefore be feasible that even far below  $T_c$  the  $Cu^{2+}$  spins are *not* paired, but rapidly exchanging. On the other hand, any model which allows for spin-carrying objects (spinons) in the superconducting state [31] (i.e., with resultant large spin susceptibility) has to deal with the fact that the nuclear spinlattice relaxation of all nuclei (not only that of Cu), decreases by several orders of magnitude below  $T_c$  [6–10, 24]. However, from a different perspective [Equation (10)], this might be explainable by a rapid increase of J below  $T_c$ .

Finally, it should be noted also that data for the <sup>89</sup>Y Knight shift [6, 32] and spin-lattice relaxation [33] behave similarly to those for Cu(2). This is not surprising, since Y is located between the Cu(2) planes and "sees" the Cu<sup>2+</sup> spins via transferred and dipolar hyperfine interaction.

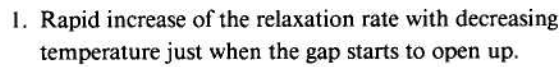
# 5. Quasiparticle excitation below and near $T_{\rm c}$ : Nuclear spin-lattice relaxation

As mentioned in the Introduction, the direct connection of quasiparticle excitation across the superconducting gap  $2\Delta$  in a BCS-like superconductor with the nuclear spin-lattice relaxation in  $^{27}$ Al was one of the key experiments in support of the BCS theory [2, 3]. The following "Hebel–Slichter features" are seen in the experimental data:





 $^{139}$ La nuclear spin-lattice relaxation rate of  $\text{La}_{1.8}\text{Sr}_{0.2}\text{CuO}_4$  in zero field versus temperature according to Seidel et al. [5]. Note the "hump" below  $T_{\rm c}^*$  and the exponential decrease for  $T < T_{\rm c}^*$  (see text).



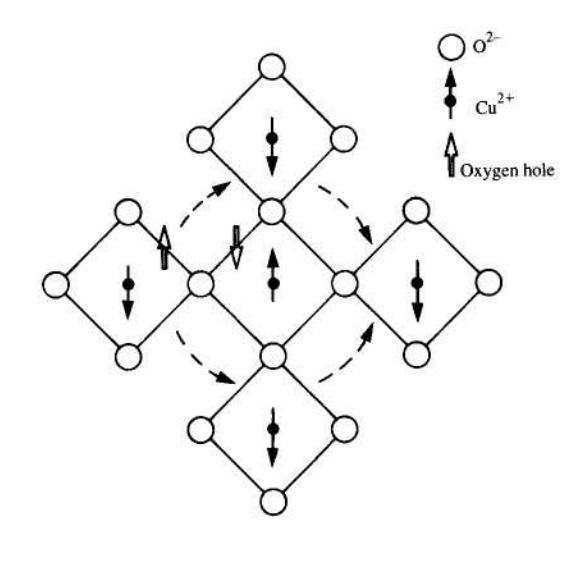
Exponential decrease of the relaxation rate with further decrease of the temperature as

$$\frac{1}{T_1} \sim \exp\left(-\Delta/kT\right) \text{ for } T \ll T_c. \tag{11}$$

The first feature is due to an increase in the density of states for quasiparticle excitation, when the gap opens at the Fermi level. Further decrease of  $1/T_1$  according to Equation (11) stems from the quasiparticle excitation energy  $2\Delta$  across the gap [34]. These Hebel-Slichter features were indeed observed recently in the zero-field relaxation of <sup>139</sup>La in La<sub>1.8</sub>Sr<sub>0.2</sub>O<sub>4</sub> [5]. Figure 10 demonstrates this behavior. Note the "hump" at  $T_c$  and the exponential decrease below, which if fitted to Equation (11) give a relative gap energy of  $2\Delta/k_BT_c = 7$  [5]. The relaxation rate can be calculated [2, 34] as follows:

 $\frac{1}{T_{1s}} = \frac{4\pi}{\hbar} \left(\frac{\gamma_n}{\gamma_e}\right)^2 K^2 \int \left(\frac{E^2 + \Delta^2}{E^2 - \Delta^2}\right) f(E)(1 - f(E)) dE, \quad (12)$ 

where f(E) is the Fermi distribution function and K is the Knight shift. Note that Equation (12) reduces to the normal Korringa relaxation in the metallic state ( $T > T_c$ ) by setting



### a Bratting & Br

Spin scenario of  $\mathrm{Cu}^{2+}$  and oxygen hole spins in the  $\mathrm{Cu}(2)$  plane of high- $T_c$  superconductors. Indirect exchange coupling between the  $\mathrm{Cu}^{2+}$  spins seems to be responsible for the Cu spin-lattice relaxation effects, whereas the oxygen hole spins seem to dominate the <sup>139</sup>La and <sup>17</sup>O nuclear spin relaxation. The correlation between  $\mathrm{Cu}^{2+}$  and oxygen hole spins is responsible for the complicated temperature dependence of nuclear spin-lattice relaxation times.

 $\Delta=0$ . Below  $T_{\rm c}$  the gap parameter  $\Delta(T)$  depends on the temperature. Equation (12) describes the basic Hebel–Slichter features. It can easily be extended to account also for an anisotropic gap. In this situation a weighted average of the gap energy is obtained, and the height of the "hump" is decreased. This could be the reason for the fairly small hump seen in  $\rm La_{1.8}Sr_{0.8}CuO_4$ .

More recently the Hebel-Slichter features have also been observed in the <sup>17</sup>O relaxation in YBa<sub>2</sub>Cu<sub>3</sub>O<sub>7</sub> [30] and even for <sup>63</sup>Cu relaxation in YBa<sub>2</sub>Cu<sub>3</sub>O<sub>6.52</sub> [35]. It should be evident that these features may be expected to appear at any nuclear site, as long as some hyperfine interaction is transferred to the corresponding nuclear spin. However, they do not reveal the location of the quasiparticles.

### 6. Conclusions

The experimental NMR results presented here suggest the following scenario, sketched in Figure 11. The  $CuO_2$  planes consist of  $Cu^{2+}$  with spin S=1/2 which are antiferromagnetically correlated. Holes with spin 1/2 are added under doping into the oxygen layers. The extent to which  $Cu^{2+}$  spins and the hole spins at the oxygen sites are coupled is difficult to assess. The temperature dependences

of nuclear spin relaxation in Cu and O seem to be related but are not identical. The Hebel-Slichter features are not seen in the copper relaxation of  $YBa_2Cu_3O_7$ , which seems to be dominated by antiferromagnetic fluctuations of the  $Cu^{2+}$ spins. On the other hand, all nuclear spin relaxation rates decrease drastically below  $T_c$ , leading us to the conclusion that either all spins become paired in the superconducting state, or the antiferromagnetic fluctuations become frozen.

This and many of the different phenomena discussed here need to be explained by a more quantitative analysis. Nevertheless, I hope to have succeeded in demonstrating the power and versatility of NMR for the investigation of high- $T_{\rm c}$  superconductors.

### **Acknowledgments**

This contribution would not have been possible without the encouragement of Alex Müller, to whom I am very grateful for supporting this research. Moreover, I want to thank my co-workers F. Hentsch and H. Seidel for their skillful assistance with the experiments. The Bundesminister für Forschung und Technologie (BMFT) provided financial support.

### References and note

- 1. J. G. Bednorz and K. A. Müller, Z. Phys. B 64, 189 (1986).
- 2. L. C. Hebel and C. P. Slichter, Phys. Rev. 113, 1504 (1959).
- 3. Y. Masuda and A. G. Redfield, Phys. Rev. 125, 159 (1962).
- D. E. MacLaughlin, in Solid State Physics, Vol. 31, Academic Press, Inc., New York, 1976, p. 1.
- 5. H. Seidel, F. Hentsch, M. Mehring, J. G. Bednorz, and K. A. Müller, *Europhys. Lett.* 5, 647 (1988).
- (a) M. Mali, D. Brinkmann, L. Pauli, J. Roos, H. Zimmermann, and J. Hulliger, *Phys. Lett. A* 124, 112 (1987); (b) M. Mali, J. Roos, and D. Brinkmann, *Physica C* 153–155, 737 (1988).
- H. Riesenmeier, Ch. Grabow, E. W. Scheidt, V. Müller, and K. Lüders, Solid State Commun. 64, 309 (1987).
- 8. W. W. Warren, R. E. Walstedt, G. F. Brennert, G. P. Espinosa, and J. P. Rameika, *Phys. Rev. Lett.* **59**, 1860 (1987).
- (a) Y. Kitaoka, S. Hiramatsu, K. Ishida, T. Kohara, Y. Oda, K. Amaya, and K. Asayama, *Physica* 148B, 298 (1987); (b) Y. Kitaoka, S. Hiramatsu, T. Kondo, and K. Asayama, *J. Phys. Soc. Jpn.* 57, 30 (1988); (c) Y. Kitaoka, S. Hiramatsu, Y. Kohori, K. Ishida, T. Kondo, H. Shibai, K. Asayama, H. Takagi, S. Uchida, H. Iwabuchi, and S. Tanaka, *Physica C* 153–155, 83 (1988).
- E. Lippmaa, E. Joon, I. Heinmaa, V. Miidel, A. Miller, R. Stern, I. Furo, L. Mihaly, and P. Banki, *Physica C* 153–155, 91 (1988).
- 11. H. Lütgemeier, Physica C 153-155, 95 (1988).
- (a) A. Abragam, Principles of Nuclear Magnetism, Oxford University Press, Oxford, U.K., 1961; (b) C. P. Slichter, Principles of Magnetic Resonance, Springer-Verlag, New York, 1978.
- C. H. Pennington, D. J. Durand, D. B. Zax, C. P. Slichter, J. P. Rice, and D. M. Ginsberg, *Phys. Rev. B* 37, 7944 (1988).
- H. Riesenmeier, J. Pattloch, K. Lüders, and V. Müller, Solid State Commun. 68, 251 (1988).
- (a) Y. Kitaoka, S. Hiramatsu, T. Kohara, K. Asayama, K. Ohishi, M. Kikuchi, and N. Kobayashi, *Jpn. J. Appl. Phys.* 26, L397 (1987);
  (b) Y. Kitaoka, K. Ishida, K. Fujiwara, K. Asayama, H. Katayama-Yoshida, Y. Okabe, and T. Takahashi, *IBM J. Res. Develop.* 33, 277 (1989, this issue).
- H. Lütgemeier and M. W. Pieper, Solid State Commun. 64, 267 (1987).

- I. Watanabe, K. Kumagai, Y. Nakamura, T. Kimura, Y. Nakamichi, and H. Nakajima, J. Phys. Soc. Jpn. 56, 3028 (1987).
- A. Aharony, R. J. Birgeneau, A. Coniglio, M. A. Kastner, and H. E. Stanley, *Phys. Rev. Lett.* 60, 1330 (1988).
- I. Watanabe, Y. Nakamura, and K. Kumagai, *Physica C* 152, 262 (1988).
- (a) F. Hentsch, H. Seidel, M. Mehring, J. Bednorz, and K. A. Müller, *Physica C* 153–155, (1988); (b) F. Hentsch et al., to be published.
- 21. H. Yasuoka, T. Shimizu, Y. Ueda, and K. Kosuge, *J. Phys. Soc. Jpn.*, in press.
- 22. H. Lütgemeier and B. Rupp, ICM Conference 1988, Paris, France.
- (a) M. Takigawa, P. C. Hammel, R. H. Heffner, Z. Fisk, J. L. Smith, and R. B. Schwarz, *Phys. Rev. B* 39, 300 (1989); (b) M. Takigawa, P. C. Hammel, R. H. Heffner, and Z. Fisk, *Phys. Rev. B (Rapid Commun.)* (1989).
- T. Imai, T. Shimizu, H. Yasuoka, Y. Ueda, and K. Kosuge, J. Phys. Soc. Jpn. 57, 2280 (1988).
- M. Mehring, in Low-Dimensional Conductors and Superconductors, NATO ASI Series, Plenum Publishing Co., New York, 1987, p. 185.
- 26. T. Moriya, J. Phys. Soc. Jpn. 18, 516 (1963).
- (a) P. W. Anderson and P. R. Weiss, Rev. Mod. Phys. 25, 269 (1953);
  (b) P. W. Anderson, J. Phys. Soc. Jpn. 9, 316 (1954);
  (c) T. Moriva, Prog. Theor. Phys. 16, 33 (1956).
- T. Moriya, *Prog. Theor. Phys.* **16**, 33 (1956). 28. Starting from  $1/T_1 = (\pi/2) (M_2^3/3M_4)^{1/2}$  (see [12(a)]) and calculating  $M_2 = (A/2)^2$ ,  $M_4 = (AJ)^2/2$  for electron spin 1/2, square lattice, and  $J \gg A$ , one arrives at Equation (10).
- (a) K. B. Lyons, P. A. Fleury, L. F. Schneemeyer, and J. V. Waszczak, *Phys. Rev. Lett.* 60, 732 (1988); (b). A. Aharony, R. J. Birgeneau, and M. A. Kastner, *IBM J. Res. Develop* 33, 287 (1989, this issue).
- Y. Kitaoka, K. Ishida, K. Asayama, H. Katayama-Yoshida, Y. Okabe, and T. Takahashi, *Nature*, in press.
- 31. P. W. Anderson, Science 235, 1196 (1987).
- 32. H. B. Brom, G. J. Kramer, J. van den Berg, and J. C. Jol, *Solid State Commun.*, in press.
- J. T. Markert, T. W. Noh, S. E. Russek, and R. M. Cotts, *Solid State Commun.* 63, 847 (1987).
- J. R. Schrieffer, Theory of Superconductivity, Benjamin, New York, 1966.
- T. Imai, H. Yasuoka, T. Shimizu, Y. Ueda, and K. Kosuge, Technical Report of ISSP, July 1988.

Received September 9, 1988; accepted for publication November 11, 1988

Michael Mehring Physikalisches Institut, Universität Stuttgart, D-7000 Stuttgart 80, Federal Republic of Germany. Professor Mehring received his Diploma in 1964 and his Doctorate in natural sciences in 1968 from Universität Münster. From 1969 to 1971 he was a Research Associate with Dr. John Waugh at the Massachusetts Institute of Technology, completing his Habilitation in 1971. From 1972 to 1981 he was Professor of Physics at the University of Dortmund, and since 1981 Full Professor of Physics at the University of Stuttgart. Professor Mehring's research interests include pulsed electron spin resonance/electron nuclear double resonance; nuclear magnetic resonance of organic conductors and high- $T_c$  superconductors; the physical principles of molecular electronics; and molecular information storage.